Electronic Supplementary Material (ESI) for New Journal of Chemistry.

Supporting Information

Naphthalimide-decorated imino-phenol: Supramolecular gelation and selective sensing of Fe^{3+} and Cu^{2+} ions under different experimental conditions

Sumit Ghosh[1], Nabajyoti Baildya[1], Narendra Nath Ghosh[2] and Kumaresh Ghosh[1]*

[1]*Department of Chemistry, University of Kalyani, Kalyani-741235, India.*
Email: ghosh_k2003@yahoo.co.in
[2]*Department of Chemistry, University of Gour Banga, Malda-732103, India*

Table S1. Results of gelation test for **1**.

Solvent	**1**
DMSO	S
DMF	S
THF	S
CH_3CN	I
CH_3OH	I
$CHCl_3$	S
Benzene	I
$CHCl_3$: CH_3OH (1:1, v/v)	P
Diethyl ether	I
Hexane	I
Petroleum ether	I
DCM	S
DMSO: H_2O (1:1, v/v)	**G (10 mg/mL)**
DMF: H_2O (1:1, v/v)	**G (8 mg/mL)**
THF: H_2O (1:1, v/v)	P
CH_3CN: H_2O (1:1, v/v)	P
Diox: H_2O (1:1, v/v)	P

S = Solution; G = Gel (mgc); I = Insoluble; P = Precipitation; Gelation was primarily investigated by inversion of vial method after 10-15 mins of sample preparation ([Gelator] = 20 mg/mL).

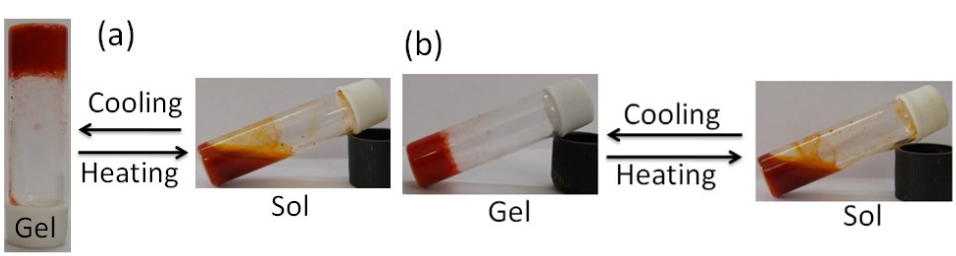

Fig. S1. Pictorial representation of the thermo reversibility of the (a) DMF- H_2O (1:1, v/v) and (b) DMSO- H_2O (1:1, v/v) gels of **1**.

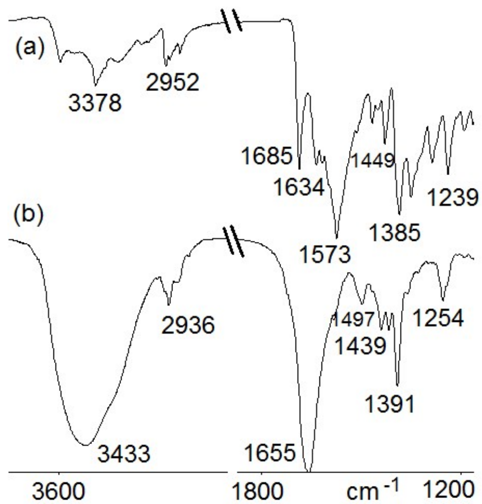

Fig. S2. Partial FTIR spectra of **1** in (a) amorphous and (b) gel state.

(a)

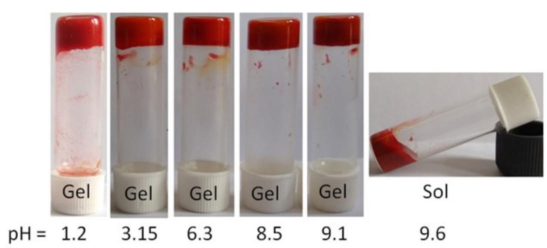

(b)

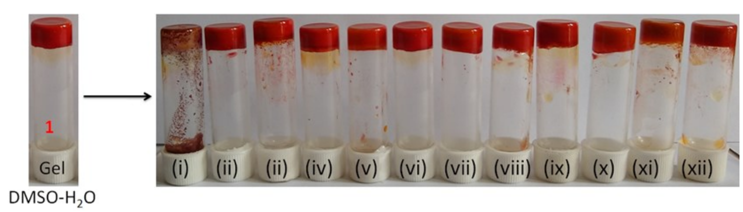

Fig. S3. Photograph showing the phase changes of DMF-H_2O (1:1, v/v) gel of **1** at different pHs; (b) Photograph showing the phase changes of DMSO-H_2O (1:1, v/v) gel of **1** (at mgc value) in the presence of 1 equiv. amount of different metal ions after 1h [(i) Fe^{3+}, (ii) Ag^{+}, (iii) Zn^{2+}, (iv) Pb^{2+}, (v) Fe^{2+}, (vi) Hg^{2+}, (vii) Co^{2+}, (viii) Ni^{2+}, (ix) Al^{3+}, (x) Cd^{2+}, (xi) Cu^{2+} and (xii) Ca^{2+} ions. Fe^{2+} and Pb^{2+} are used as perchlorate salts and others are as nitrate salts].

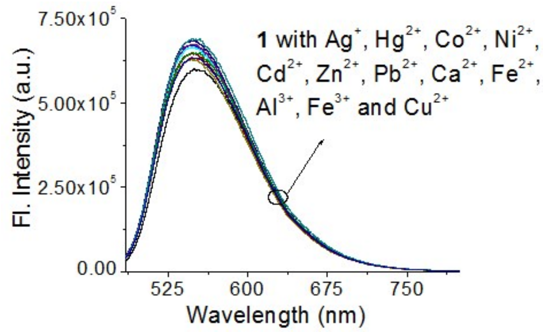

Fig. S4. Change in emission of compound **1** (c = 2.5 x 10^{-5} M) upon addition of different metal ions (c = 1 x 10^{-3} M in DMF-H_2O (1:1, v/v).

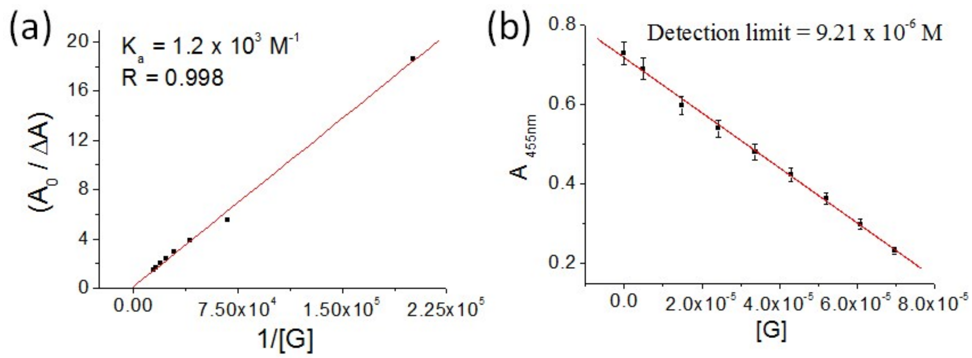

Fig. S5. (a) Benesi–Hildebrand plot and (b) detection limit of **1** (c = 2.5 x 10^{-5} M) for Cu^{2+} ion at 455 nm (c = 1.0 x 10^{-3} M) in CH_3CN from UV-vis titration.

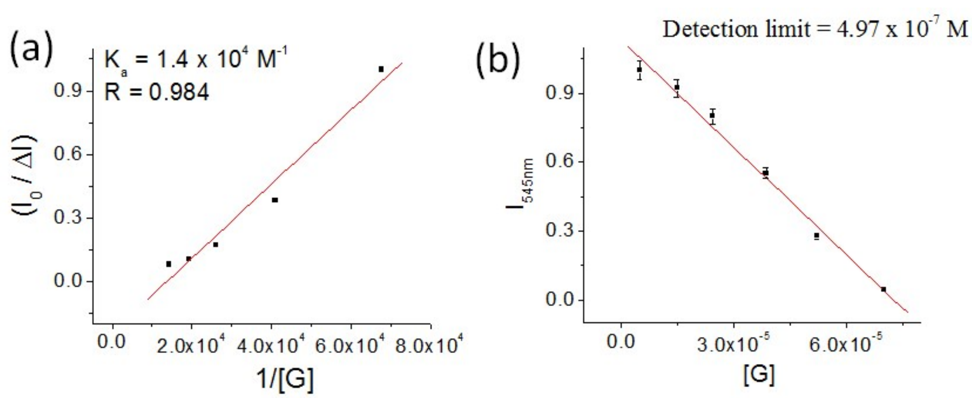

Fig. S6. (a) Benesi–Hildebrand plot and (b) detection limit of **1** (c = 2.5 x 10^{-5} M) for Cu^{2+} ion at 545 nm (c = 1.0 x 10^{-3} M) in CH_3CN from fluorescence titration.

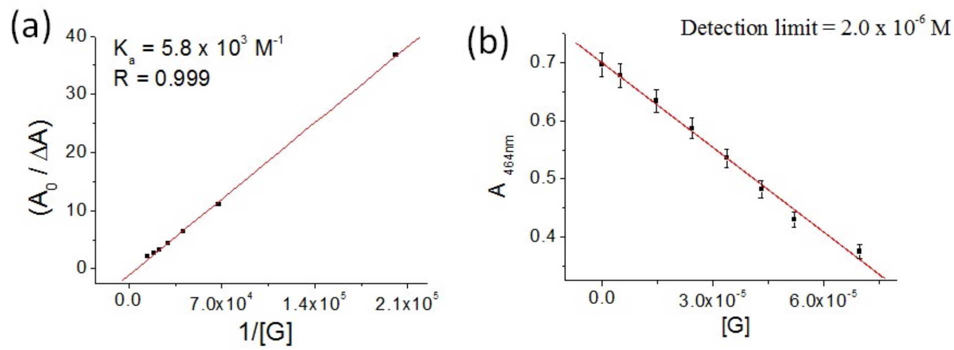

Fig. S7. (a) Benesi–Hildeband plot, (b) detection limit of **1** (c = 2.5 x 10^{-5} M) for Cu^{2+} ion at 464 nm (c = 1.0 x 10^{-3} M) in CH_3CN: H_2O (4:1, v/v) from UV-vis titration.

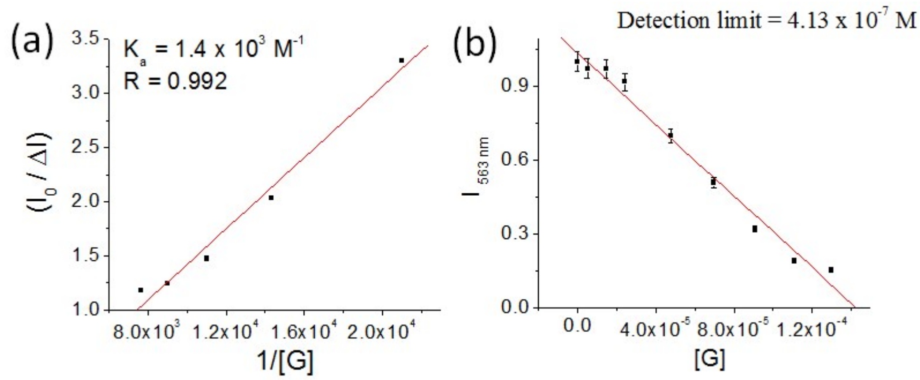

Fig. S8. (a) Benesi–Hildebrand plot and (b) detection limit of **1** (c = 2.5 x 10^{-5} M) for Cu^{2+} ion at 563 nm (c = 1.0 x 10^{-3} M) in CH_3CN: H_2O (4:1, v/v) from fluorescence titration.

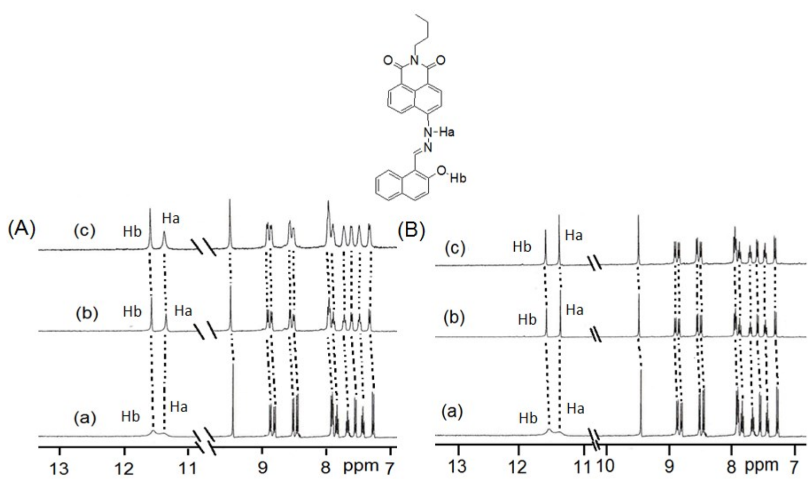

Fig. S9. Partial ^1H NMR (400 MHz, d_6-DMSO) of (A) (a) compound **1** (c = 6.8 × 10^{-3} M), (b) **1** with 1 equiv. $Cu(ClO_4)_2$ and (c) **1** with 2 equiv. $Cu(ClO_4)_2$ and (B) (a) compound **1** (c = 6.8 × 10^{-3} M), (b) **1** with 1 equiv. $Fe(ClO_4)_3$ and (c) **1** with 2 equiv. $Fe(ClO_4)_3$.

Table S2. Simulated absorption wavelengths (λ_{max} in nm), oscillator strengths (***f***), and the composition of the corresponding electronic transitions (H = HOMO; L = LUMO) calculated using B3LYP/6-31g(d) for non aggregated forms and B3LYP-D3 dispersion corrected hybrid function for aggregated forms.

Compound	λ_{max}	***f***	**ε (10⁴)**	**Main compositions (contribution)**
1 in DMF	352 (expt)	0.28	2.84	H→L+3 (87%)
	423 (expt)	0.35	2.36	H-2→L (66%), H→L+1 (25%)
	648 (expt)	0.56	1.54	H→L (100%)
1 in DMF-1H_2O	492 (473)[a]	0.74	2.03	H→L (99%)
1 in DMF-2H_2O	500 (473) [a]	0.78	1.99	H→L (99%)
1 aggregated DMF-H_2O	432 (448)[a]	0.51	2.31	H→L (57%), H→L+1 (41%)
1 aggregated water bridging DMF-H_2O	433 (448) [a]	0.27	2.31	H-1→L (47%), H→L+1 (38%)
1 in CH_3CN	479 (473)[a]	0.77	2.08	H→L (99%)
1 with Cu^{2+} in CH_3CN	497 (473)[a]	0.12	2.01	H-2→L (18%), H→L (20%), H→L+1 (28%)

Table S3: Reported structures for Cu^{2+} sensing in solution phase by imino-phenol compounds.

Entry	**Structure of sensor**	**Detection media**	**solvent**	**Detection limit**	**Interference from other metal ions**	**Ref.**
1	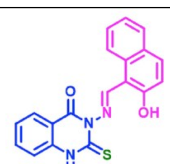	solution	DMSO:H_2O (1:9, v/v)	20 nM	-	1

2	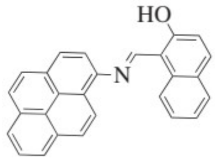	Solution	DMSO:H_2O (8:2, v/v)	2.17×10^{-6} M 3.19×10^{-6} M	 Fe^{3+}	2
3	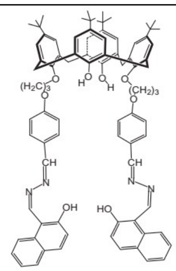	Solution	CH_3CN	-	-	3
4	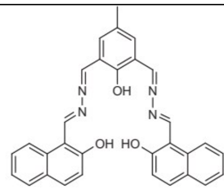	Solution	CH_3CN:H_2O (8:2, v/v)	5×10^{-6} M	-	4
5	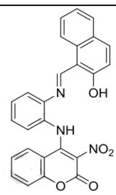	Solution	CH_3CN:H_2O (2:3, v/v)	2.95×10^{-5} M	-	5
6	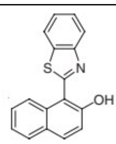	Solution	CH_3CN	2×10^{-6} M	-	6
7	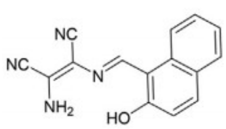	Solution	DMSO:H_2O (3:7, v/v)	2.4×10^{-6}M	-	7
8	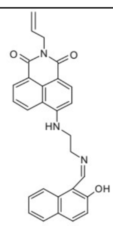	Solution	THF:H_2O (9:1, v/v)	1×10^{-6} M	-	8
9	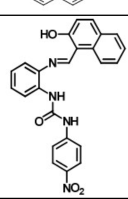	Solution	CH_3CN	-	-	9

10	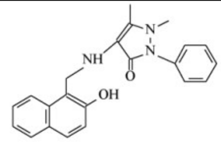	Solution	Aqueous solution	-	-	10
11	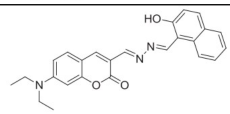	Solution	MeOH:H_2O (6:4, v/v)	1 ×10^{-5} M	-	11
12	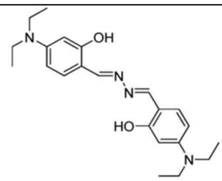	Solution	CH_3CN	9.8 ×10^{-7} M	Fe^{3+}	12
13	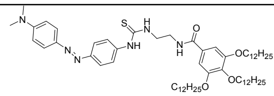	Solution	CH_3CN	5.99 ×10^{-9} M	Fe^{3+}, Hg^{2+}	13
14	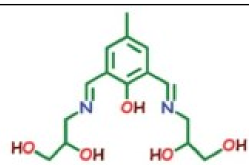	Solution	Tris-buffer (25 mM, pH = 7.4) solution	11.2 nM	-	14
15	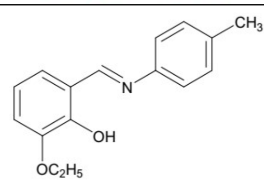	Solution	EtOH:H_2O (3:1, v/v)	-	-	15
This work	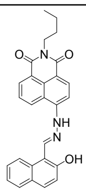	Solution	CH_3CN:H_2O (4:1, v/v)	4.13 x 10^{-7} M	-	-

Table S4: Reported structures for Fe^{3+} sensing in gel phase.

Entry	Gelator structure	Detection media	solvent	Sensing mechanism	Interference from other metal ions	Ref.
1	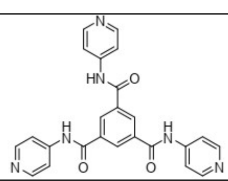	Gel	H_2O	Sol to gel transition	Fe^{2+}	16

2	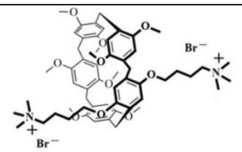	Gel	H_2O	Fluorescence OFF Gel-to-Gel state	-	17
3	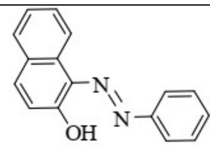	Gel	CH_3CN:H_2O (1:1, v/v)	Visual detection through gel-to sol transition	Cu^{2+}	18
4	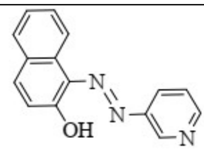	Gel	CH_3CN:H_2O (1:1, v/v)	Visual detection through gel-to sol transition	-	18
5	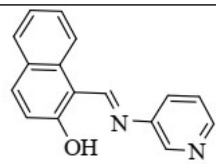	Gel	DMSO:H_2O (1:1, v/v)	Visual detection through color change	-	18
6	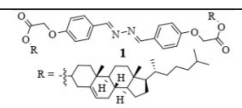	Gel	$CHCl_3$:MeOH (3:1, v/v)	Visual detection through sol-to gel transition	Ag^+	19
7	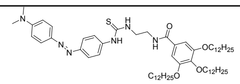	Gel	CH_3CN	Visual detection through gel-to gel transition	Hg^{2+}, Cu^{2+}	13
8	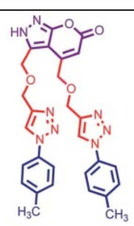	Gel	MeOH	Visual detection through gel-to gel transition	-	20

This work	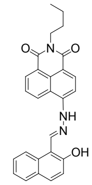	Gel	DMF:H_2O (1:1, v/v)	Visual detection through Gel-to sol transition	Fe^{3+}	-

^{1}H NMR ($CDCl_3$ with 1 drop d_6-DMSO, 400 MHz) of 1

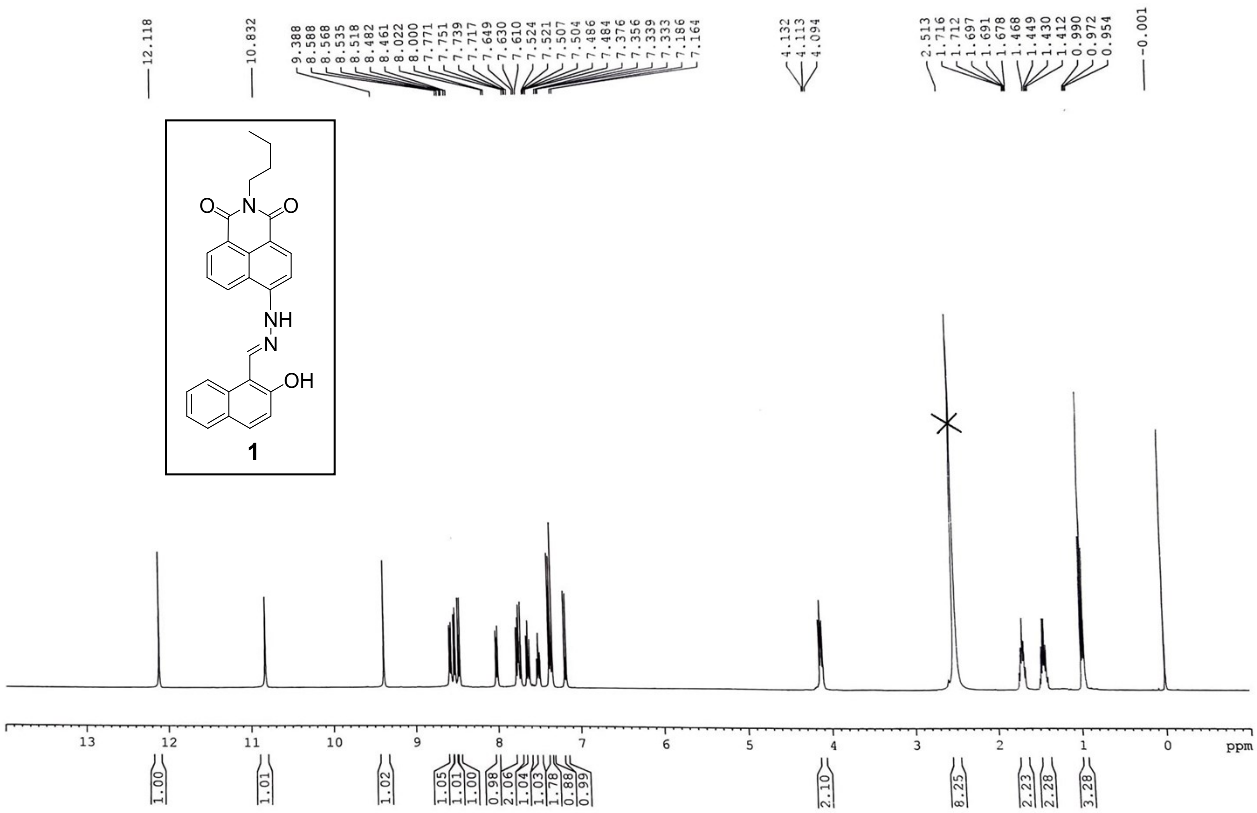

^{13}C NMR ($CDCl_3$ with 1 drop d_6-DMSO, 100 MHz) of 1

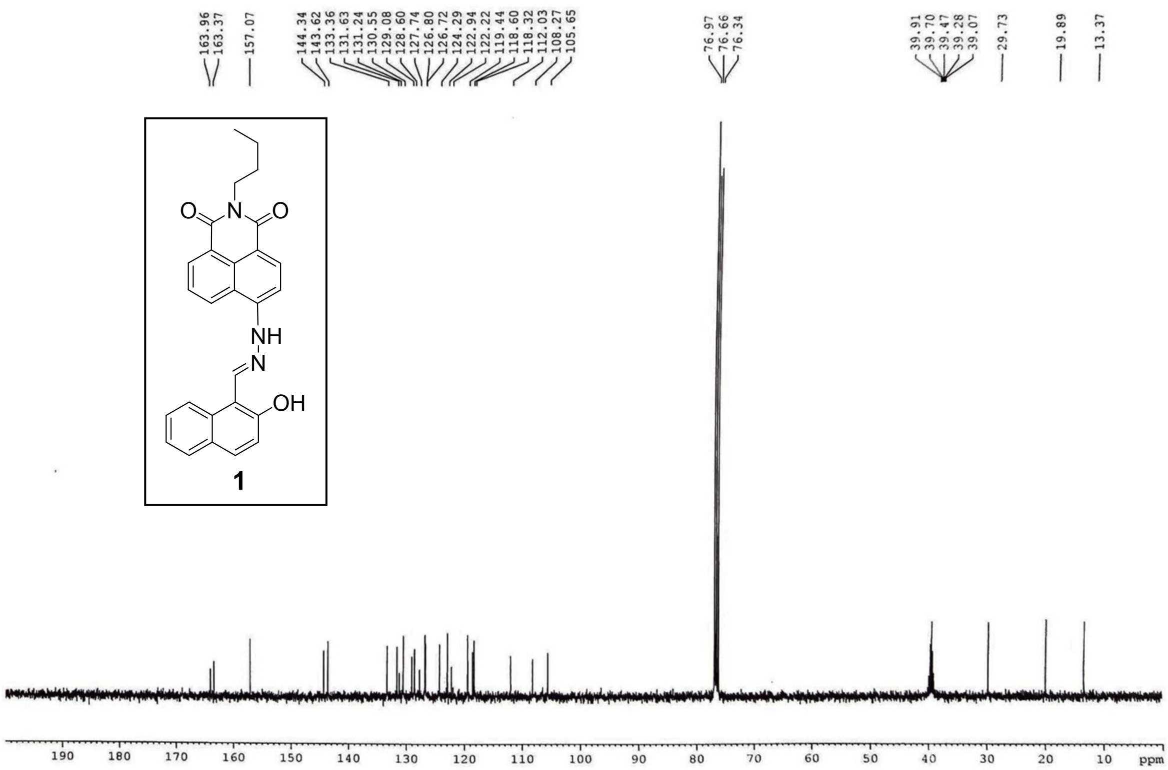

Mass spectrum of 1.

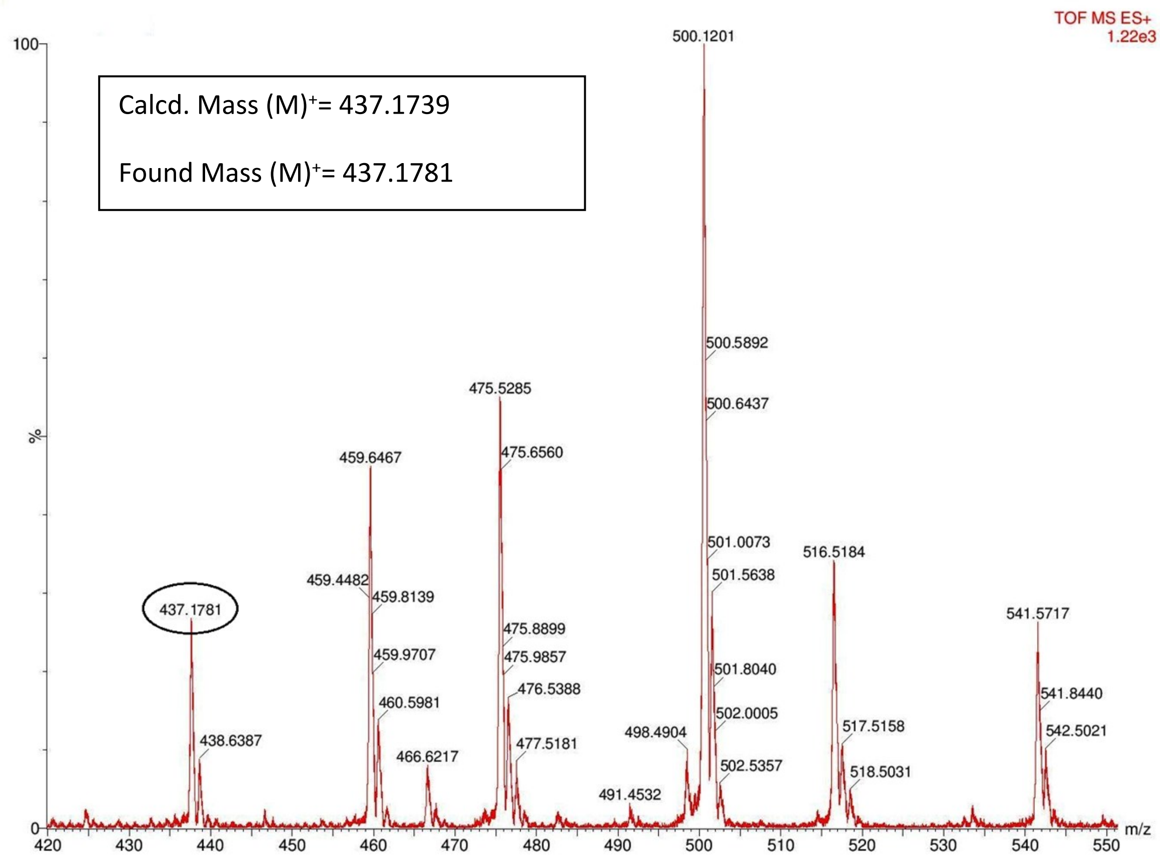

Reference

1. T. Anand, G. Sivaraman and D. Chellappa, *J. Photochem. Photobiol. A*, 2014, **281**, 47.
2. Y. R. Bhorge, H. T. Tsai, K. F. Huang, A. J. Pape, S. N. Janaki, Y. P. Yen, *Spectrochim Acta A.*, 2014, **130**, 7.
3. H. M. Chawla, P. Goel and P. Munjal, *Tetrahedron Lett*., 2015, **56**, 682.
4. S. Goswami, S. Maity, A. K. Das and A. C. Maity, *Tetrahedron Lett*., 2013, **54**, 6631.
5. J. HY, P. GJ, N. YJ, C. YW, Y. GR and K. C, *Dyes. Pigm*., 2014, **109**, 127.
6. N. Kaura, J. Singha, G. Dhaka, R. Rani and V. Luxami, *Supramol. Chem.,* 2015, **27**, 453.
7. S. A. Lee, J. J. Lee, J. W. Shin, K. S. Min and C. Kim, *Dyes. Pigm*., 2015, **116**, 131.
8. N. Singh, N. Kaur, B. McCaughan and J. F. Callan, *Tetrahedron Lett*., 2010, **51**, 3385.
9. P. Singh, H. Singh, G. Bhargava and S. Kumar*, J. Mater. Chem. C*, 2015, **3**, 5524.
10. J. S. Wu, P. F. Wang, X. H. Zhang and S. K. Wu, *Spectrochim Acta. A,* 2006, **65**, 749.
11. H. Xu, X. Wang, C. Zhang, Y. Wu and Z. Liu, *Inorg. Chem. Commun.*, 2013, **34**, 8.
12. N. Narayanaswamy and T. Govindaraju, Sensor Actuat. B-Chem., 2012, **161**, 304.
13. X. Cao, Y. Li, Y. Yu, S. Fu, A. Gao and X. Chang, Nanoscale, 2019, **11**, 10911.
14. B. Naskar, R. Modak, D. K. Maiti, A. Bauzá, A. Frontera, P. K. Maiti, S. Mandal and S. Goswami, *RSC Adv.*, 2017, **7**, 11312.
15. G. T. Tigineh and L.-K. Liu, *Bull. Chem. Soc. Ethiop.*, 2017, **31**, 31.
16. J. –L. Zhong, X. –J. Jia, H. –J. Liu, X. –Z. Luo,S. –G. Hong, N. Zhanga and J. –B. Huang, *SoftMatter*, 2016, **12**, 191.
17. J.–F. Chen, Q. Lin, H. Yao, Y. –M. Zhang and T. –B. Wei, *Mater. Chem. Front.*, 2018, **2**, 999.
18. A. Panja and K. Ghosh, *Mater. Chem. Front.*, 2018, **2**, 1866.
19. A. Panja and K. Ghosh, *Mater. Chem. Front.*, 2018, **2**, 2286.
20. H. Jain, N. Deswal, A. Joshi, C. N. Ramachandran and R. Kumar, *Anal. Methods*, 2019, **11**, 3230.